EMERGING ADVANCES IN INTEGRATED TECHNOLOGY
e-ISSN: 2773-5540

EmAIT

Vol. 5 No. 1 (2024) 7-15
https://publisher.uthm.edu.my/ojs/index.php/emait

The Potential of Gold Nanobipyramids as Anti-Fungal for Dermatophytes Fungi at Living Animals

Khor Wing Kang[1], Marlia Morsin[1,2]*, Nur Liyana Razali[1,2]

[1] *Faculty of Electrical & Electronic,*
Universiti Tun Hussein Onn Malaysia, Parit Raja, Batu Pahat, 86400, Johor, MALAYSIA

[2] *Microelectronics & Nanotechnology –Shamsuddin Research Centre (MiNT-SRC),*
Institute for Integrated Engineering,
Universiti Tun Hussein Onn Malaysia, Parit Raja, Batu Pahat, 86400, Johor, MALAYSIA

*Corresponding Author: marlia@uthm.edu.my
DOI: https://doi.org/10.30880/emait.2024.05.01.002

Article Info

Received: 12 January 2024
Accepted: 13 June 2024
Available online: 30 June 2024

Keywords

Nanoparticles, gold nanobipyramids, seed-mediated growth method, dermatophytes, fungi treatment, concentration

Abstract

Dermatophytes are a group of fungi that cause dermatophytosis, a type of skin infection affecting both humans and animals. While dermatophytosis is typically self-limiting, it can pose significant challenges for individuals with weakened immune systems. Additionally, current treatment options for dermatophytosis have their limitations, including issues of toxicity, inefficacy, and the emergence of drug-resistant strains. Recently, nanotechnology-based approaches have emerged as a promising strategy to overcome the drawbacks of conventional antifungal medications. Gold Nanoparticles (GNPs) have demonstrated substantial antifungal activity against various fungal species, including dermatophytes. Among these, Gold Nanobipyramids (GNBPs) exhibit unique physicochemical properties that enhance their effectiveness against dermatophytes. GNBPs were synthesized using the Seed-Mediated Growth Method (SMGM) due to its simplicity. Optically, GNBPs displayed plasmonic peaks at 1.548 (wavelength 561 nm) and 2.372 (wavelength 807 nm). Structurally, intensity peaks at 38.15° (plane 111) and 44.49° (plane 200) were identified. GNBPs have a surface density of ~70.227±0.530. In the dermatophyte treatment process, GNBPs exhibited varying inhibitory effects. At 40% concentration, fungal growth persisted, with a surface density similar to the no control area. At 60%, inhibition occurred, though less efficiently. The most effective inhibition was observed at 80%, and complete inhibition was achieved at 100% concentration. GNBPs proved successful in inhibiting fungal growth, attributed to their curvature and sharp edges interacting with microbial cell membranes, leading to membrane damage and cellular content leakage.

1. Introduction

Gold nanoparticles are microscopic particles made of gold atoms that have a diameter of less than 100 nanometers [1]. They have unique properties that are different from bulk gold, such as a high surface area-to-volume ratio, outstanding thermal and electrical conductivity, and unique optical properties such as strong absorption and scattering of light, as well as being biocompatible and having low toxicity [2,3]. Moreover, gold nanoparticles have unique properties that make them beneficial in a wide range of fields, including biology, electronics, catalysis, and environmental science. They are also utilized in biomedicine for instance, in medication delivery, imaging, and cancer therapy [4].

Ringworm, caused by dermatophyte fungi, poses a significant health concern for animals, including domestic pets like cats [5]. These fungi, belonging to the *genera Trichophyton*, *Microsporum*, and *Epidermophyton*, not only affect the skin but can also lead to systemic infections in immunocompromised individuals [6]. The transmission of dermatophytes can occur through direct contact with an infected animal or through contact with contaminated surfaces, such as grooming tools or bedding. Dermatophytes have evolved unique mechanisms to adapt to their host environment. Their preference for keratin as a nutrient source enables them to thrive on the outer layers of the skin, where keratin is abundant [7]. This adaptation involves the secretion of keratinolytic enzymes, such as proteases and keratinases, enabling the fungi to break down and utilize the structural proteins of the host's tissues.

In the scope of combating dermatophytes, the use of Gold Nanobipyramids (GNBPs) introduces a novel and promising approach. Beyond their distinct physical properties, GNBPs exhibit excellent stability and biocompatibility, making them suitable candidates for biomedical applications. The curvature and sharp edges of GNBPs are anticipated to interact effectively with microbial cell membranes, leading to membrane damage and disruption of cellular processes, ultimately inhibiting fungal growth. The disc diffusion method, a standard procedure in antimicrobial susceptibility testing, is employed in this study to assess the inhibitory potential of GNBPs against dermatophytes. Different concentrations of GNBPs are applied to ascertain the most effective concentration for inhibiting fungal growth. This research not only addresses the challenges posed by conventional antifungal medications, such as toxicity and drug resistance, but also explores the multifaceted applications of nanotechnology in the field of veterinary medicine.

2. Methodology

Phase I of the flowchart focuses on the fabrication of gold nanoparticles into bipyramid shapes. The process is divided into two main parts: the synthesis and characterization of the gold nanoparticles, as illustrated in Fig. 1(a). In the synthesis process, two steps are involved: seeding and growth. The seeding step begins by introducing a gold precursor, such as gold chloride, into a solution. This precursor serves as the source for the gold nanoparticles. Then, a reducing agent is added to the solution to initiate the formation of seed nanoparticles. The seed nanoparticles act as the nucleation sites for further growth. Once the seeding step is complete, the growth process begins. Additional gold precursors and a reducing agent are added to the solution containing the seed nanoparticles. This leads to the controlled growth of the nanoparticles, resulting in the desired bipyramid shape. In addition, various parameters, such as temperature, reaction time, and concentrations, are carefully controlled to achieve the desired shape and size of the gold nanoparticles.

Phase II of the flowchart focuses on the characterization of the synthesized gold nanoparticles. Four properties are analyzed: physical, structural, optical, and morphological properties, as illustrated in Fig. 1(a). These properties provide important insights into the nature and behavior of the nanoparticles. To analyze the physical properties, techniques such as size distribution analysis and surface charge measurements may be employed. This helps determine the average size of the nanoparticles and their stability in the solution. The structural properties of the gold nanoparticles are typically analyzed using X-ray diffraction (XRD). XRD provides information about the crystal structure, phase composition, and lattice parameters of the nanoparticles. The optical properties of the nanoparticles, including their absorption and scattering behavior, are often characterized using UV-Vis spectroscopy. This technique used for determination of the nanoparticles' absorption spectra and provides information about their surface plasmon resonance. Morphological properties refer to the shape, size, and surface characteristics of the nanoparticles. Field-emission scanning electron microscopy (FESEM) is commonly used to observe the nanoparticles at high magnification and obtain detailed information about their morphology.

Phase III of the flowchart involves the treatment process of dermatophytes fungi using the disc diffusion method, as illustrated in Fig. 1(b). The disc diffusion method is a well-known technique used to assess the antimicrobial activity of substances. In this case, the effectiveness of the GNBPs in treating dermatophytes fungi needs to be evaluated. For this method, the experiment includes six controls: no control, positive control and 40, 60, 80 & 100 % concentration of GNBPs from growth solution. The no control group serves as a baseline, while the positive control group contains a known effective antifungal agent. The GNBPs will be applied to the fungal samples, and observations are made to determine their effect on inhibiting the growth of the fungi. Hence, the results obtained from Phase III will indicate whether the GNBPs exhibit antimicrobial properties against the dermatophytes fungi. This information is beneficial for realizing the potential application of gold nanoparticles in fungal treatment.

3. Results and Discussion

After Gold Nanobipyramids (GNBPs) have been successfully synthesized and characterized in previous experimental phases, which are Phase I and Phase II experiments that involved the synthesis and characterization of these nanomaterials using specific methods and techniques. The focus of this part is on the

Emerging Advances in Integrated Technology Vol. 5 No. 1 (2024) p. 7-15

characterization of GNBPs synthesized using the Seed Mediated Growth Method (SMGM) and the subsequent result of their physical, optical, morphological, and structural properties. After the GNBPs growth solution was synthesized and characterized, in dermatophytes fungi treatment process was also accomplished (Phase III), which included the variation concentrations of GNBPs growth solution has been examined using disc diffusion method as well as the result of dermatophytes fungi treatment by using disc diffusion method also discussed in this part.

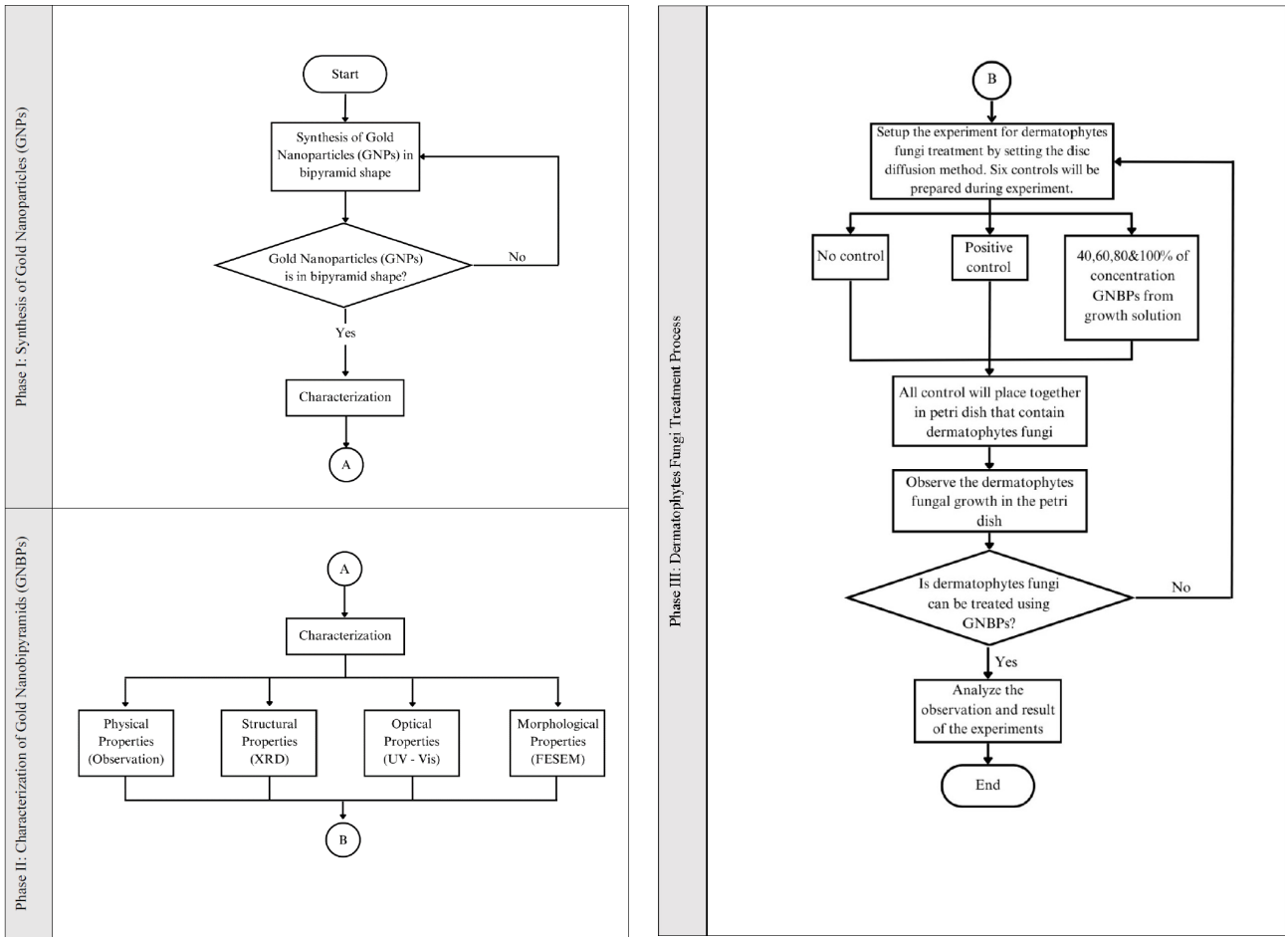

(a) **(b)**

Fig. 1 *Overall experimental process (a) Part 1; (b) Part 2*

3.1 Physical Observation of Synthesized Seed and Growth Solution

The colour change observed in the seed solution is due to the formation of gold nanoparticles (GNPs). When Gold Chloride reacts with Chloroplatinic Acid Hydrate, it undergoes a reduction reaction facilitated by the Sodium Borohydride present in the solution. This reduction reaction leads to the formation of gold atoms from gold ions, resulting in the generation of gold nanoparticles. The yellow colour of the seed solution is a characteristic feature of the formation of GNPs. The interaction between the gold ions and the Hexadecyltrimethylammonium Bromide (CTAB) molecules in the solution results in the stabilization of the gold nanoparticles. CTAB acts as a surfactant and forms a bilayer around the nanoparticles, preventing them from aggregating and maintaining their stability.

During the addition of ice-cold Sodium Borohydride, the borohydride anion acts as a reducing agent. It donates electrons to the gold ions, leading to further reduction and growth of the gold nanoparticles. As the size of the nanoparticles increases, the plasmon resonance peak shifts from the yellow range to the brown range, resulting in the observed colour change from yellow to brown. In summary, the colour changes in the seed solution from yellow to brown are attributed to the reduction of gold ions to GNPs by the action of sodium borohydride and the stabilization of these nanoparticles with the CTAB bilayer, as illustrated in Fig. 2(a).

Next, to initiate the growth process of GNBPs in the growth solution, several chemicals are utilized. The growth solution is prepared by combining six different chemicals: gold chloride, CTAB, chloroplatinic acid, hydrochloric acid, ascorbic acid, and the seed solution obtained from the previous step. The preparation of the growth solution involves mixing 20 mL of 0.1 M CTAB with 0.875 mL of 0.01 M gold chloride, 0.025 mL of 0.01 M

chloroplatinic acid, 0.2 mL of 0.01 M hydrochloric acid, and 0.4 mL of 1.0 M hydrochloric acid. This mixture results in a yellow-coloured solution due to the displacement of ions by gold chloride in the CTAB micelles. The gold ions are effectively incorporated into the CTAB micelles, leading to the formation of GNPs. The next step involves adding 0.16 mL of 0.1 M ascorbic acid to the mixture solution. This addition causes a colour change from yellow to colourless. The ascorbic acid reduces the bound gold ions (Au(I)) in the CTAB micelles, facilitating the formation of gold nanoparticles.

(a) **(b)**

Fig. 2 *GNBPs solutions (a) Seed solution; (b) Growth solution*

Finally, 50 µL of the seed solution, containing stabilized gold nanoparticles, is introduced into the growth solution. The mixture is stirred for 1 minute to ensure thorough mixing. Over time, the colour of the growth solution gradually shifts from colourless to purple. This colour change signifies the ongoing growth process of gold nanoparticles within the solution, as illustrated in Fig. 2(b). To conclude, the growth solution is prepared by combining various chemicals, including gold chloride, CTAB, chloroplatinic acid, hydrochloric acid, and ascorbic acid. The addition of the seed solution initiates the growth process, resulting in a colour change from colourless to purple as the GNBPs continue to develop.

3.2 Optical Characterization of GNBPs

The UV-Vis spectrometer is utilized for the optical characterization of the synthesized gold Gold Nanobipyramids (GNBPs). By analyzing the UV-Vis graphs obtained, the localized surface plasmon resonance (LSPR) response of these nanoparticles can be determined, as illustrated in Fig. 3. Next, the UV-Vis graph for GNRs displays two distinct peaks, namely the longitudinal surface plasmonic resonance (l-SPR) and the transverse surface plasmonic resonance (t-SPR). These peaks are a result of the dimensions of the bipyramids. The lower-energy peak corresponds to the t-SPR and is influenced by the length of the bipyramids. On the other hand, the higher-energy peak corresponds to the l-SPR and is affected by the diameter of the bipyramids.

Similarly, the UV-Vis graph for GNBPs exhibits two peaks, indicating the presence of localized surface plasmon resonance. The lower-energy peak corresponds to the t-SPR and is associated with the dimensions of the bipyramid, particularly its length. The higher-energy peak corresponds to the l-SPR and is influenced by the diameter of the bipyramid. The UV-Vis graph of GNBPs presented in Fig. 3 provides comprehensions into their optical properties. The spectrum shows two prominent peaks, namely the transverse surface plasmonic resonance (t-SPR) and the longitudinal surface plasmonic resonance (l-SPR). The t-SPR peak is observed at a wavelength of 561 nm with an intensity of 1.548. This peak indicates the resonant absorption of light by the transverse dimension of the GNBPs. The intensity measurement reflects the strength or magnitude of the absorption at this specific wavelength. On the other hand, the l-SPR peak appears at a longer wavelength of 807 nm with an intensity of 2.372. This peak corresponds to the resonant absorption of light by the longitudinal dimension of the GNBPs. The higher intensity of the l-SPR peak suggests a relatively stronger absorption compared to the t-SPR peak. The distinct t-SPR and l-SPR peaks in the UV-Vis spectrum of the GNBPs demonstrate their characteristic surface plasmon resonances.

Emerging Advances in Integrated Technology Vol. 5 No. 1 (2024) p. 7-15

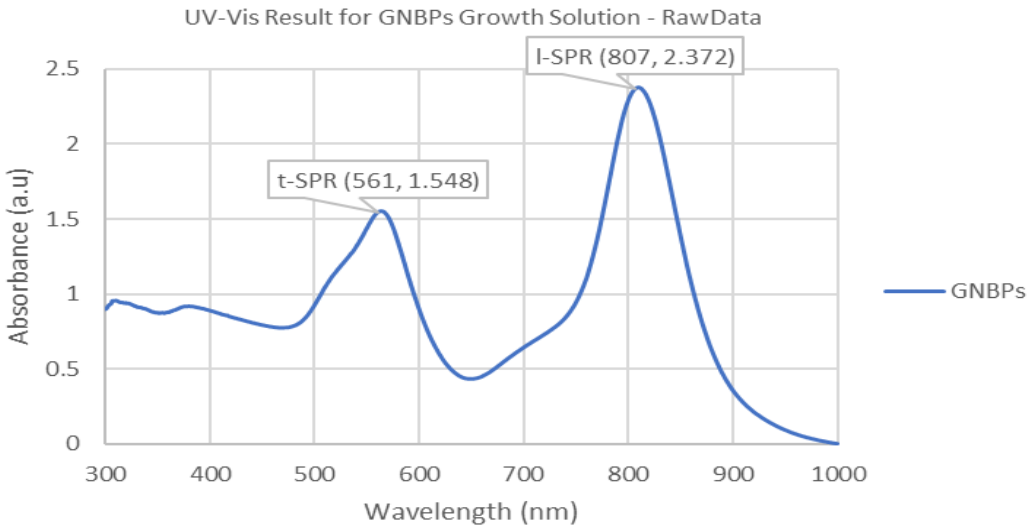

Fig. 3 *Uv-Vis graph of result for GNBPs*

3.3 Morphological Characterization of GNBPs

The morphological characterization of the synthesized Gold Nanobipyramids (GNBPs) was conducted using Field-Emission Scanning Electron Microscopy (FESEM) images. This characterization aimed to determine the shape of the successfully synthesized GNBPs, which were confirmed to be in the form of bipyramids, as illustrated in Fig.4 (a-c).

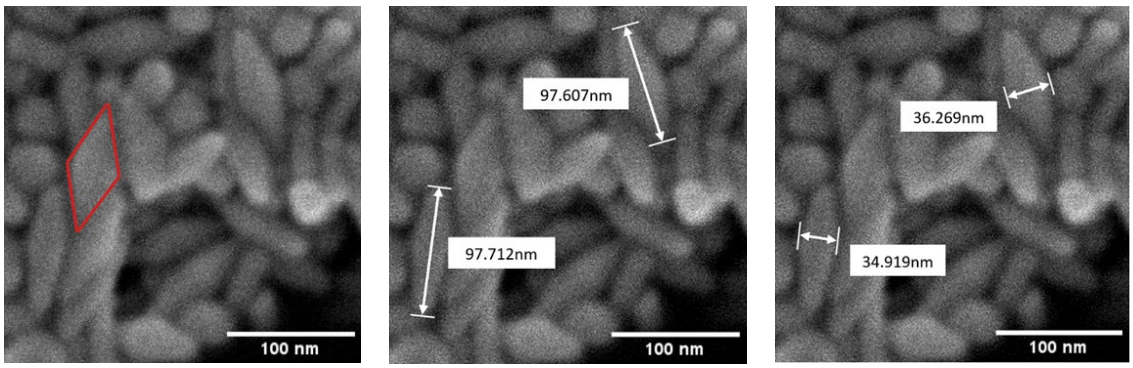

(a) **(b)** **(c)**

Fig. 4 *Geometry and size of GNBPs (a) Bipyramid shaped; (b) Length of GNBPs; (c) Diameter of GNBPs*

3.4 Structural Characterization of GNBPs

The GNBPs were subjected to X-Ray Diffraction (XRD) analysis to characterize their structure. XRD helps determine the chemical composition and arrangement of atoms within the composite material on the glass substrate. The XRD patterns obtained for both the GNRs and GNBPs samples were carefully analyzed. The patterns presented in Fig. 5, contain distinct peaks that correspond to the diffraction of X-rays by the crystal lattice of the nanoparticles. These peaks provide essential information about the crystalline structure and the presence of specific crystallographic planes within the nanoparticles. By inspecting the XRD patterns, the chemical composition of the GNBPs can be identified. Different crystal phases exhibit characteristic peak positions, known as 2θ angles, which can be used to determine the specific crystal structures present in the samples.

Based on Fig. 5, the XRD result for GNBPs indicates two intensity peaks corresponding to the crystallographic planes (111) and (200) at diffraction angles of 38.15° and 44.49°, respectively. The intensity at the angle of 38.15° is recorded as 409, while the intensity at the angle of 44.49° is reported as 207.

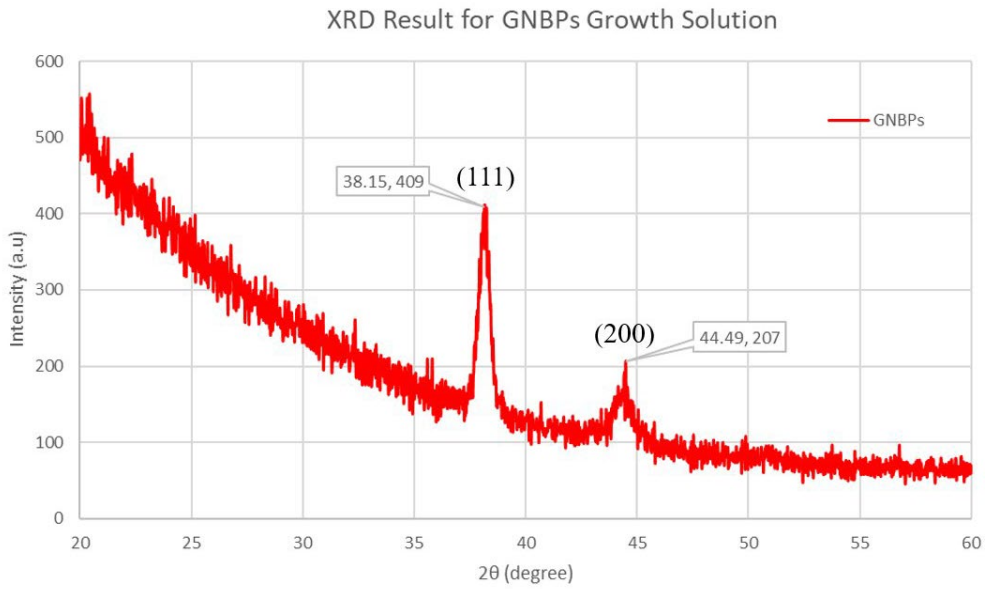

Fig. 5 *XRD graph of result for GNBPs*

3.5 Variation of Concentration of GNBPs from Growth Solution

As discussed in methodology, the experiment includes six controls: no control, positive control and 40, 60, 80 & 100 % concentration of GNBPs from growth solution. The variation of concentration of nanoparticles in the colloidal solution is crucial to examine the efficiency of anti-fungal growth. Thus, the generated different concentration of GNBPs solutions as shown in Fig. 6, each different concentration GNBPs solution has 2.5ml as stock for dermatophytes treatment purposes by using disc diffusion method.

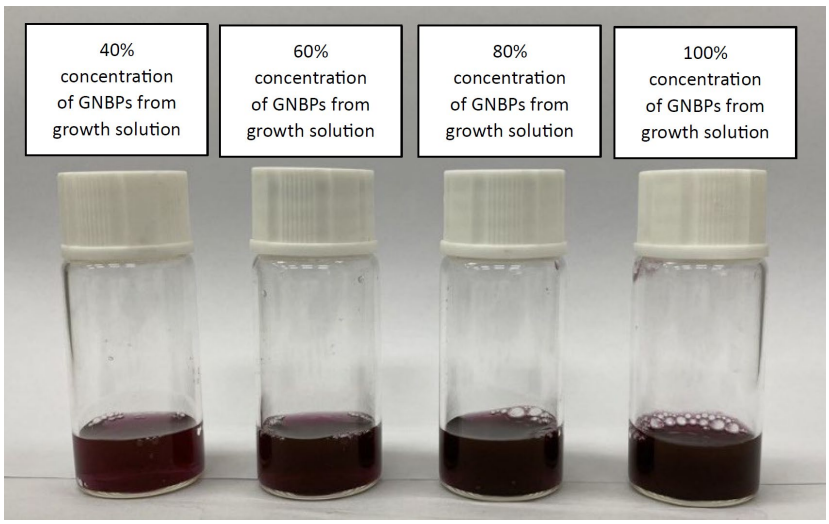

Fig. 6 *Different concentrations of GNBPs solutions*

3.6 Observation of Gold Nano Bipyramids as Anti-fungal

Regarding the area around disc and agar, the results obtained under the magnification X500 from microscope depicted the microscopic observations in the vicinity of the disc control. Two sets of results were acquired through microscopic analysis, encompassing (A1) No control, (B1) Positive control, (C1) 40% concentration of GNBPs, (D1) 60% concentration of GNBPs, (E1) 80% concentration of GNBPs, and (F1) 100% concentration of GNBPs, as illustrated in Fig. 7(a). Additionally, a second set of results was obtained for (A2) No control, (B2) Positive control, (C2) 40% concentration of GNBPs, (D2) 60% concentration of GNBPs, (E2) 80% concentration of GNBPs, and (F2) 100% concentration of GNBPs, showcased in Fig. 7(b).

Emerging Advances in Integrated Technology Vol. 5 No. 1 (2024) p. 7-15

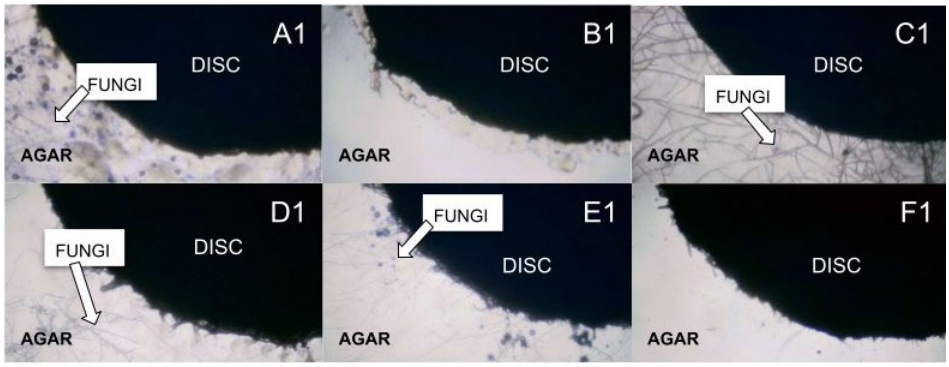

(A1) No control. (B1) Positive control. (C1) 40% concentration of GNBPs.
(D1) 60% concentration of GNBPs. (E1) 80% concentration of GNBPs. (F1) 100% concentration of GNBPs.

(a)

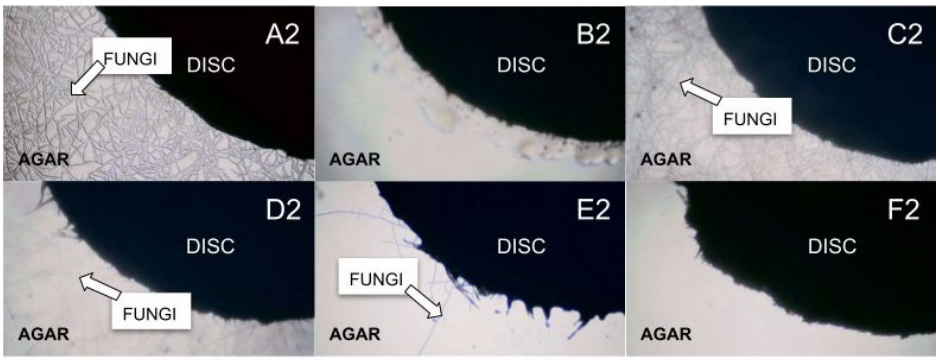

(A2) No control. (B2) Positive control. (C2) 40% concentration of GNBPs.
(D2) 60% concentration of GNBPs. (E2) 80% concentration of GNBPs. (F2) 100% concentration of GNBPs.

(b)

Fig. 7 *The result of disc diffusion method under microscope (a) Batch 1; (b) Batch 2*

Based on the results from Fig. 7 (a) and (b), the uncontrolled fungal spread within the designated area in the No control group (A1&A2) underscores the importance of implementing control measures. Without any inhibitory agent, dermatophytes fungi proliferated without constraint, emphasizing the necessity for intervention. In contrast, the absence of fungal spread in the designated area for the Positive control group (B1&B2) highlights the effectiveness of the known antifungal agent. The positive control successfully inhibited the growth of dermatophytes fungi in this specific region, validating its efficacy. Moreover, the examination of the 40% concentration of GNBPs (C1&C2) reveals fungal spread in the area, indicating that at this concentration, GNBPs were not entirely effective in preventing the proliferation of dermatophytes fungi. The visualization suggests a partial inhibitory effect at this concentration. Moving on to the 60% concentration of GNBPs (D1&D2), while fungal spread is observed in the area, the extent is slightly smaller compared to the 40% concentration (C1&C2). This suggests a partial inhibitory effect, indicating that the 60% concentration of GNBPs may have some inhibitory impact on fungal growth. Notably, at the 80% concentration of GNBPs (E1&E2), a significant decrease in fungal presence around the area is observed compared to the 60% concentration (D1&D2). This indicates a concentration-dependent response, suggesting that higher concentrations of GNBPs may lead to a more pronounced reduction in fungal growth. In the case of the 100% concentration of GNBPs (F1&F2), the absence of fungal spread around the area suggests a potent inhibitory effect. At this concentration, GNBPs appear to be highly effective in preventing the proliferation of dermatophytes fungi, showcasing their potential as a robust antifungal agent.

3.7 Assessment of Dermatophytes Fungal Surface Density in The Vicinity of the Disc and Agar Area

In order to visualize the results in a quantitative manner, the surface density of fungi for Batch 1 and Batch 2 was recorded across various controls and concentrations, as presented in Fig. 8 (a) and (b), respectively. These figures outline the average surface density of dermatophytes fungi in the vicinity of the disc and agar area, which created an overview of the inhibitory effects of different concentrations of GNBPs.

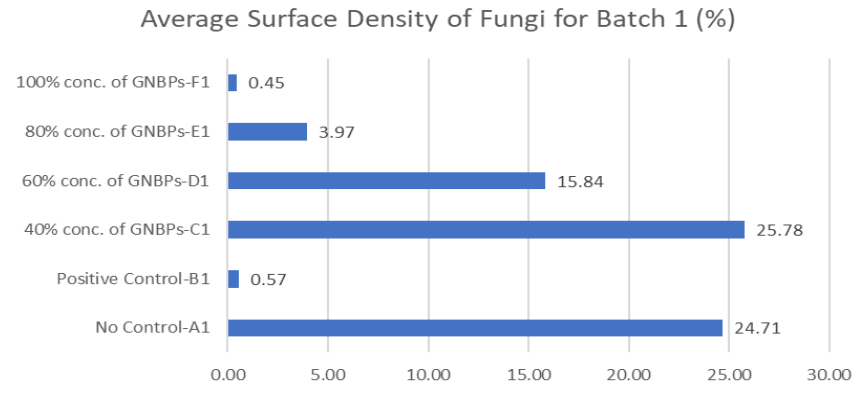

(a)

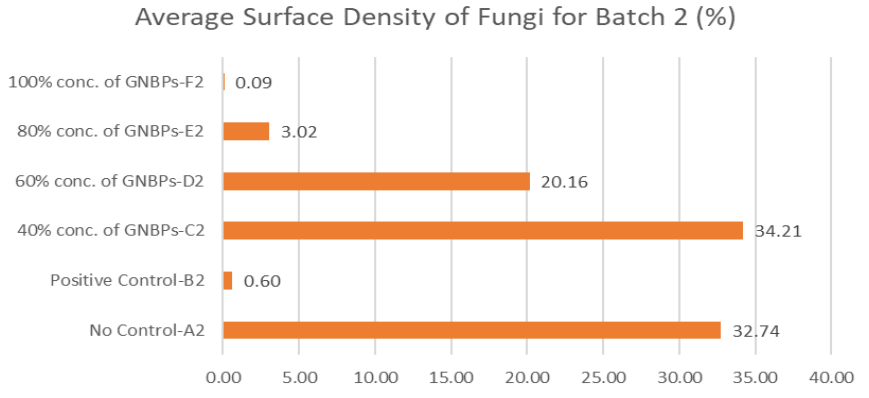

(b)

Fig. 8 *Average surface density of fungi (a) Batch 1; (b) Batch 2*

The assessment of dermatophytes fungal surface density in the vicinity of the disc and agar area yielded insightful findings. Notably, the No Control groups (A1 & A2) exhibited the highest average surface density, emphasizing the uncontrolled proliferation of fungi in the absence of any inhibitory agent. This underscores the critical need for control measures in preventing the unchecked spread of dermatophytes fungi. Conversely, the Positive Control groups (B1 & B2) displayed remarkably low average surface density values, reaffirming the efficacy of the known antifungal agent in inhibiting fungal growth. These results serve as a crucial baseline for evaluating the relative performance of GNBPs at different concentrations. Moving on to the 40% concentration of GNBPs (C1 & C2), the average surface density values indicate a partial inhibitory effect. While GNBPs at this concentration demonstrated some ability to curb fungal proliferation, the surface density values suggest that it may not be entirely effective in preventing the spread of dermatophytes fungi.

At the 60% concentration of GNBPs (D1 & D2), a noticeable reduction in average surface density is observed compared to the 40% concentration. This signifies a concentration-dependent response, suggesting that higher concentrations of GNBPs may indeed result in a more substantial inhibitory impact on dermatophytes fungi growth. The trend continues with the 80% concentration of GNBPs (E1 & E2), where a significant decrease in average surface density is evident. This reinforces the notion that higher concentrations of GNBPs correlate with a more pronounced reduction in fungal presence, indicating a concentration-dependent effectiveness. Notably, at the 100% concentration of GNBPs (F1 & F2), the average surface density values approach near-zero levels. This suggests a potent inhibitory effect, where GNBPs at full concentration effectively suppress the growth of dermatophytes fungi in the designated area. To conclude, it is evident that concentrations of GNBPs impacts the efficiency in inhibiting dermatophytes fungi, in which, the higher the concentration, the lower the surface density of fungi.

4. Conclusion

To summarize, regarding the first objective of this study, which involved synthesizing Gold Nanobipyramids (GNBPs) by using the Seed Mediated Growth Method (SMGM) has been successfully accomplished. The initial phase (Phase I) of the synthesis involved the preparation of seeding and growth solutions. This step was carried out effectively, allowing for the subsequent growth of GNBPs. Regarding the characterization of the GNBPs to determine their physical, structural, optical, and morphological properties were also successfully achieved in

(Phase II). Through various analytical techniques and instruments, the properties of the GNBPs were thoroughly examined and documented. In detail, for optical properties, the plasmonic peak GNBPs, the highest absorption peak is 1.548 for t-SPR at wavelength 561 nm and 2.372 at wavelength 807 nm. For structural properties, the intensity peak at plane (111) for GNRs and GNBPs occur at 38.15° while for plane (200) occur at 44.49°. For morphological properties, the surface density for GNBPs is 70.2269±0.0531.

Next, the second objective was also achieved, the application of GNBPs in treating dermatophytes fungi using the disc diffusion method was effectively carried out in (Phase III). The experimental setup and treatment process showcased the inhibition of fungal growth in the presence of GNBPs. Microscopic observations from the disc diffusion test result also demonstrated the varying degrees of inhibitory effects at different concentrations of GNBPs. Lastly, the exploration of the effect of GNBPs concentration in fungi treatment, which constitutes the third objective, was thoroughly investigated and achieved. The concentration of GNBPs in the growth solution was estimated, and the disc diffusion test result demonstrated their potential as effective antifungal agents against dermatophytes fungi. The quantitative assessment of fungal surface density in the vicinity of the disc and agar area given important information into the concentration-dependent response of GNBPs in inhibiting dermatophytes fungi. The observed trends in surface density clearly indicated that higher concentrations of GNBPs led to more pronounced reductions in fungal presence, aligning with the anticipated outcomes.

In conclusion, the study underscores the promising potential of GNBPs as versatile nanomaterials with applications in medicine, particularly in the development of efficient antifungal agents. The findings open avenues for further research and development in nanotechnology for combating fungal infections and contribute to the broader field of nanomedicine.

Acknowledgement

The research and work are supported in terms of facilities provided by Microelectronics & Nanotechnology-Shamsuddin Research Centre (MiNTSRC), UTHM. The authors also would like to thank the Faculty of Electrical and Electronic Engineering, UTHM for its support.

Conflict of Interest

Authors declare that there is no conflict of interests regarding the publication of the paper.

Author Contribution

The authors confirm contribution to the paper as follows: ***study conception and design:*** *Khor Wing Kang, Marlia Morsin;* ***data collection:*** *Khor Wing Kang;* ***analysis and interpretation of results:*** *Khor Wing Kang, Marlia Morsin, Nur Liyana Razali;* ***draft manuscript preparation:*** *Khor Wing Kang, Marlia Morsin. All authors reviewed the results and approved the final version of the manuscript.*

References

[1] Zaleska-Medynska, A. (2022). *What are Nanoparticles? Definition, Size, Uses and Properties - TWI*. TWI Ltd. https://www.twi-global.com/technical-knowledge/faqs/what-are-nanoparticles

[2] Jain, P. K., Lee, K. S., El-Sayed, I. H., & El-Sayed, M. A. (2006). Calculated Absorption and Scattering Properties of Gold Nanoparticles of Different Size, Shape, and Composition: Applications in Biological Imaging and Biomedicine. *Journal of Physical Chemistry B*, *110*(14), 7238–7248. https://doi.org/10.1021/JP0571700

[3] Alkilany, A. M., & Murphy, C. J. (2010). Toxicity and cellular uptake of gold nanoparticles: what we have learned so far? *Journal of Nanoparticle Research*, *12*(7), 2313–2333. https://doi.org/10.1007/S11051-010-9911-8

[4] Hammami, I., Alabdallah, N. M., jomaa, A. Al, & kamoun, M. (2021). Gold nanoparticles: Synthesis properties and applications. *Journal of King Saud University - Science*, *33*(7), 101560. https://doi.org/10.1016/J.JKSUS.2021.101560

[5] Miller, W. (2023). *Ringworm: A Serious but Readily Treatable Affliction*. Cornell University College of Veterinary Medicine. https://www.vet.cornell.edu/departments-centers-and-institutes/cornell-feline-health-center/health-information/feline-health-topics/ringworm-serious-readily-treatable-affliction

[6] Ghannoum, M. A., & Isham, N. C. (2009). Dermatophytes and dermatophytoses. In *Clinical Mycology* (2nd Ed, pp. 375–384). https://doi.org/10.1016/B978-1-4160-5680-5.00016-5

[7] Ciesielska, A., Kawa, A., Kanarek, K., Soboń, A., & Szewczyk, R. (2021). Metabolomic analysis of Trichophyton rubrum and Microsporum canis during keratin degradation. *Scientific Reports*, *11*(1), 3959. https://doi.org/10.1038/S41598-021-83632-Z